

# Velocity segregation effects in galaxy clusters at $0.4 \lesssim z \lesssim 1.5$

S. Barsanti<sup>1</sup>, M. Girardi<sup>1,2</sup>, A. Biviano<sup>2</sup>, S. Borgani<sup>1,2,3</sup>, M. Annunziatella<sup>2</sup>, and M. Nonino<sup>2</sup>

<sup>1</sup> Dipartimento di Fisica, Università degli Studi di Trieste, via Tiepolo 11, I-34143 Trieste, Italy

<sup>2</sup> INAF–Osservatorio Astronomico di Trieste, via G. B. Tiepolo 11, I-34133, Trieste, Italy

<sup>3</sup> INFN–Sezione di Trieste, via Valerio 2, I-34127 Trieste, Italy

Received 27 May 2016/ Accepted 11 August 2016

## ABSTRACT

**Aims.** Our study is meant to extend our knowledge of the galaxy color and luminosity segregation in velocity space (VCS and VLS, resp.), to clusters at intermediate and high redshift.

**Methods.** Our sample is a collection of 41 clusters in the  $0.4 \lesssim z \lesssim 1.5$  redshift range, for a total of 4172 galaxies, 1674 member galaxies within  $2R_{200}$  with photometric or spectroscopic information, as taken from the literature. We pay attention to perform homogeneous procedures to select cluster members, compute global cluster properties, in particular the LOS velocity dispersion  $\sigma_v$ , and separate blue from red galaxies.

**Results.** We find evidence of VCS in clusters out to  $z \simeq 0.8$  (at the 97%-99.99% c.l., depending on the test), in the sense that the blue galaxy population has a 10-20% larger  $\sigma_v$  than the red galaxy population. Poor or no VCS is found in the High- $z$  sample at  $z \geq 0.8$ . For the first time, we detect VLS in non-local clusters and confirm that VLS only affects the very luminous galaxies, with brighter galaxies having lower velocities. The threshold magnitude of VLS is  $\sim m_3 + 0.5$ , where  $m_3$  is the magnitude of the third brightest cluster galaxy, and current data suggest that the threshold value moves to fainter magnitudes at higher redshift. We also detect (marginal) evidence of VLS for blue galaxies.

**Conclusions.** We conclude that the segregation effects, when their study is extended to distant clusters, can be important tracers of the galaxy evolution and cluster assembly and discuss the poor/no evidence of VCS at high redshift.

**Key words.** galaxies: clusters: general – galaxies: kinematics and dynamics – galaxies: evolution – cosmology: observations

## 1. Introduction

It is well established that the properties of cluster galaxies differ from those of field galaxies and that clusters are characterized by radial gradients. Galaxies in denser, central regions are usually of earlier morphological type, redder color, and lower star formation rate. This is the well-known phenomenon of the spatial segregation of spiral/elliptical galaxies and of blue/red galaxies in local and distant clusters (e.g., Melnick & Sargent 1977; Dressler 1980; Whitmore et al. 1993; Abraham et al. 1996; Dressler et al. 1999; Gerken et al. 2004). More recently, this effect is only questioned at very high redshift where some authors detect an inversion of the star formation rate vs. galaxy density (Tran et al. 2010; Santos et al. 2015, but see Ziparo et al. 2014). The spatial segregation is a basic observable in the framework of galaxy evolution and, in particular, of the connection between galaxy evolution and cluster environment.

A related phenomenon is the segregation of galaxies of different color/type in velocity space (hereafter VCS). Unfortunately, requiring a lot of observational effort to measure galaxy redshifts, this effect is far less known than the spatial segregation. Since the pioneering works of Tammann (1972) and Moss & Dickens (1977), several studies have reported significant differences in the velocity distributions of different galaxy populations. The velocity dispersion of the population of blue, star-forming galaxies is found to be larger than that of the population of red, passive galaxies (e.g., Sodré et al. 1989; Biviano et al. 1992; Scodreggio et al. 1995; Biviano et al. 1996;

Colless & Dunn 1996; Mohr et al. 1996; Biviano et al. 1997; Adami et al. 1998; Dressler et al. 1999; Goto 2005).

Moss & Dickens (1977) suggested that VCS is an evidence of an infalling population of field galaxies into the clusters. Large data samples, obtained stacking galaxies of several clusters, have allowed to trace the velocity dispersion profiles (VDPs) and obtain new insights on the issue. Biviano et al. (1997) analyzed the ESO Nearby Abell Cluster Survey (ENACS – 107 clusters, see Katgert et al. 1996) and inferred that the kinematical segregation of the emission line galaxies (ELGs) with respect to the passive galaxy population reflects the time of infall rather than the virialized condition. In fact, they found that the VDP of ELGs is consistent with the fact that ELGs are on more radial orbits than passive galaxies. Carlberg et al. (1997) analyzed the Canadian Network for Observational Cosmology cluster sample (CNOC – 16 clusters at medium redshift  $z \sim 0.3$ , see Yee et al. 1996), finding that the blue galaxy population is characterized by a larger value of the global velocity dispersion than the red galaxy population and a different VDP. The difference in the VDP is an expected consequence of the fact that both populations trace the same cluster potential with different spatial density profiles. Biviano & Katgert (2004) have shown that early and late spectroscopic type galaxies of ENACS clusters are in equilibrium in the cluster potential and that late-type galaxies have more radially-elongated orbits. Some interesting papers have started to analyze cluster numerical simulations in the attempt to trace galaxies during their infall into clusters and relate galaxy properties to their position in the projected phase space or to the kinematical properties of the galaxy population, that is velocity distribution and velocity dispersion (e.g., Mahajan et al.

Send offprint requests to: S. Barsanti, e-mail: stefania.jess@gmail.com

2011; Hernández-Fernández et al. 2014; Haines et al. 2015). In this context, VCS is therefore an important observational feature related to galaxy evolution during cluster assembly.

The presence of VCS is questioned in a few past and recent studies. Analyzing a sample of six clusters, Zabludoff & Franx (1993) found that the early- and late-type galaxies have no different velocity dispersions. The analysis of the Cluster and Infall Region Nearby Survey (CAIRNS – 8 clusters at  $z < 0.05$ , see Rines et al. 2003) have shown that the kinematics of star-forming galaxies in the infall region closely matches that of absorption-dominated galaxies (Rines et al. 2005). Hwang & Lee (2008) investigated the orbital difference between early-type and late-type galaxies in ten clusters using data extracted from SDSS and 2dFGRS data, in four of these they have not found any difference. Rines et al. (2013) analyzed the Hectospec Cluster Survey (HeCS – 58 clusters with  $0.1 \leq z \leq 0.3$ ) obtaining that the determination of velocity dispersion and dynamical mass is insensitive to the inclusion of bluer members and that the velocity dispersion of the ensemble cluster of all galaxies is only 0.8% larger than that of the red-sequence galaxies.

The above-mentioned discrepancies can be probably understood taking into account that the analysis of VCS implies several difficulties and possible sources of confusion. The member selection is particularly critical since the effect of including typically blue, field galaxies can bias the velocity dispersion of the blue population towards higher values. Another difficulty is that the amount of VCS, detected so far, is quantitatively small, accounting for  $\sim 10$ -20% (30% at most) of the value of the velocity dispersion. For a small velocity segregation, there is a strong spatial segregation and a decreasing trend of the VDP, in particular in the case of star-forming galaxies (Biviano & Katgert 2004). The last two effects combine in such way to hide the VCS effect when computing global values of the velocity dispersion, in spite of the positive detection in the VDP (e.g., Girardi et al. 2015). Indeed, most of the existing positive detections of VCS have been derived analyzing the VDPs of ensemble clusters obtained stacking together galaxies of many clusters. The price to be paid for the large gain in statistics when using ensemble clusters is that one averages away possible individual behaviors, that might explain the discrepancies above reported. Recent and ongoing cluster catalogs, based on hundreds of member galaxies per cluster (e.g., Owers et al. 2011), will allow us to study the VDP and VCS of individual clusters. MACS J1206.2-0847 is the first cluster of the CLASH-VLT survey (Rosati et al. 2014) where VCS has been analyzed (Girardi et al. 2015).

Moreover, to date, little is known about the velocity segregation in relation to cluster properties. For instance, the relation between VCS and cluster dynamical status has been explored in very few studies (Ribeiro et al. 2010; Ribeiro et al. 2013). The member selection might be particularly critical in very active clusters, and the scenario is made more complex by the fact that cluster mergers might also enhance star formation in galaxies (e.g., Caldwell & Rose 1997; Ferrari et al. 2005; Owen et al. 2005). The dependence of VCS with redshift is poorly investigated, too. The pioneering study of Biviano & Poggianti (2009), based on 18 clusters of the ESO Distant Cluster Survey (EDisCS –  $z \sim 0.4$ -0.8, see White et al. 2005), indicates that VCS is not as pronounced as in local ENACS clusters. Crawford et al. (2014) analyzed five distant clusters ( $0.5 < z < 0.9$ ) finding that red sequence, blue cloud, and green valley galaxies have similar velocity distributions. To probe of VCS in distant clusters is of interest also in view of the spectroscopic survey to be provided by the ESA Euclid mission (Laureijs et al. 2011). Euclid will provide

spectroscopic data for distant clusters at  $0.8 < z < 1.8$ , but only for galaxies with H $\alpha$  lines (Sartoris et al. 2016 and refs. therein). This raises the question as to how velocity dispersions measured using star forming galaxies compare with those usually measured with red galaxies. Understanding possible biases in the measurements of velocity dispersions using different galaxy populations has implication for cosmological applications of the distribution function of velocity dispersions (e.g., Borgani et al. 1997).

This paper is devoted to the study of VCS in distant clusters ( $0.4 \lesssim z \lesssim 1.5$ ) and is based on the data of 41 clusters collected in the literature. To obtain further insights into the physical processes involved in the velocity segregation, we also analyzed the possible presence of luminosity segregation in velocity space (VLS) which is reported in the literature as a minor effect with respect to VCS (Chincarini & Rood 1977; Biviano et al. 1992 and refs. therein). In particular, Biviano et al. (1992) have found that only the most luminous galaxies are segregated in velocity, with brighter galaxies having lower velocities. This result has been confirmed in more recent papers (Adami et al. 1998; Goto 2005; Ribeiro et al. 2013) and in poor group environments (Girardi et al. 2003; Ribeiro et al. 2010). The observed phenomenology has been explained by physical processes that transfers kinetic energy from more massive galaxies to less massive ones. In particular, the dynamical friction (Sarazin 1986) is the most probable mechanism (Biviano et al. 1992; Mahajan et al. 2011).

The paper is organized as follows. We present our cluster catalog in Sect. 2. Sections 3 and 4 are devoted to the presentation of member selection, main cluster properties, and separation between red and blue galaxy populations. Section 5 concentrates on the analysis of the VCS and VLS effects, discussed in the following Sect. 6. We give our summary and conclusions in Sect. 7.

Unless otherwise stated, we give errors at the 68% confidence level (hereafter c.l.). Throughout this paper, we use  $H_0 = 70 \text{ km s}^{-1} \text{ Mpc}^{-1}$  in a flat cosmology with  $\Omega_0 = 0.3$  and  $\Omega_\Lambda = 0.7$ .

## 2. Data sample

We collected data for clusters with redshift  $z \gtrsim 0.4$  and sampled by at least 20 galaxies with measured  $z$  in the cluster field. In order to separate late-type/blue/star-forming galaxies from early-type/red/passive galaxies, we also required color or spectral information. In most cases we used the color information and, in the following, we refer to the two above classes of galaxies as blue and red galaxies. In the data collection we also made use of NED<sup>1</sup> looking for cluster data until 2015 June 5. We only considered clusters with homogeneous data samples, that is clusters coming from one author or one collaboration. Table 1 lists the 41 clusters which pass our requirements (see the end of Sect. 4). The cluster catalog samples the redshift range 0.39-1.46 with a median redshift of 0.58 (see Fig. 1) and is a collection of 4172 galaxies, 100 galaxies per cluster (median value).

For each cluster, Table 1 lists the name of the cluster (Col. 1); the redshift as listed in the literature (Col. 2); the available magnitude information (Col. 3); the number of galaxies with measured redshift in the field,  $N_z$  (Col. 4); the sampling radius  $R_{\text{sam}}$ , in units of  $R_{200}$  (Col. 5); the redshift and magnitude references (Col. 6). The sampling radius, which is based on the estimates

<sup>1</sup> The NASA/IPAC Extragalactic Database (NED) is operated by the Jet Propulsion Laboratory, California Institute of Technology, under contract with the National Aeronautics and Space Administration.

**Table 1.** Cluster sample.

Cluster name	$z_{\text{cl,lit}}$	Mag	$N_z$	$R_{\text{sam}}/R_{200}$	Refs.
MS 0015.9+1609	0.5481	$g, r$	111	0.92	6
CL 0024+1652	0.3928	$g, r$	130	0.66	4
RX J0152.7–1357	0.8370	$r, K_s$	219	0.57	3
MS 0302.5+1717	0.4249	$R, I$	43	0.36	7
MS 0302.7+1658	0.4245	$g, r$	96	0.79	5
CL 0303+1706	0.4184	$g, r$	84	0.85	4
MS 0451.6–0305	0.5398	$g', r', i', z'$	70	0.40	12
RDCS J0910+5422	1.1005	$V, R, i, z, K$	156	2.06	18
CL 0939+4713	0.4060	$g, r$	132	0.53	4
CL J1018.8–1211	0.4734	$B, V, I$	71	0.92	15,21
CL J1037.9–1243a	0.4252	$V, R, I$	131	0.97	15,21
CL J1037.9–1243	0.5783	$V, R, I$	131	1.08	15,21
CL J1040.7–1155	0.7043	$V, R, I$	119	1.36	10,21
CL J1054.4–1146	0.6972	$V, R, I$	108	1.13	10,21
CL J1054.7–1245	0.7498	$V, R, I$	100	1.46	10,21
MS 1054.4–0321	0.8307	$V, i$	145	0.61	19
CL J1059.2–1253	0.4564	$B, V, I$	85	1.05	15,21
CL J1103.7–1245a	0.6261	$V, R, I$	178	2.25	15,21
CL J1103.7–1245	0.9580	$V, R, I$	178	2.30	20,21
RX J1117.4+0743	0.4850	$g', r'$	75	0.32	1
CL J1138.2–1133a	0.4548	$V, R, I$	112	1.42	15,21
CL J1138.2–1133	0.4796	$V, R, I$	112	0.91	15,21
CL J1216.8–1201	0.7943	$V, R, I$	118	0.78	10,21
RX J1226.9+3332	0.8908	$r', i', z'$	119	0.62	12
XMMU J1230.3+1339	0.9745	$r, i, z$	23	4.54	8,13
CL J1232.5–1250	0.5414	$B, V, I$	94	0.51	10,21
RDCS J1252–2927	1.2370	$R, K_s$	227	1.18	2
CL J1301.7–1139a	0.3969	$B, V, I$	87	1.47	15,21
CL J1301.7–1139	0.4828	$B, V, I$	87	0.73	15,21
CL J1324+3011	0.7560	$B, V, R, I$	181	0.75	14
CL J1353.0–1137	0.5882	$B, V, I$	68	1.05	15,21
CL J1354.2–1230	0.7620	$V, R, I$	126	1.41	15,21
CL J1411.1–1148	0.5195	$B, V, I$	78	0.71	15,21
3C 295	0.4593	$g, r$	35	0.16	4
CL 1601+4253	0.5388	$g, r$	98	0.78	4
CL J1604+4304	0.8970	$B, V, R, I$	96	0.89	16
CL J1604+4321	0.9240	$B, V, R, I$	135	1.06	16
MS 1621.5+2640	0.4275	$g, r$	262	2.04	5
RX J1716.6+6708	0.8090	$r, i, z$	37	0.61	9
XMMXCS J2215.9–1738	1.4570	$I, K_s$	44	3.30	11
XMMU J2235.3–2557	1.3900	$J, K_s$	179	1.74	17

**References.** (1) Carrasco et al. (2007); (2) Demarco et al. (2007); (3) Demarco et al. (2010); (4) Dressler et al. (1999); (5) Ellingson et al. (1997); (6) Ellingson et al. (1998); (7) Fabricant et al. (1994); (8) Fassbender et al. (2011); (9) Gioia et al. (1999); (10) Halliday et al. (2004); (11) Hilton et al. (2010); (12) Jørgensen & Chiboucas (2013); (13) Lerchster et al. (2011); (14) Lubin et al. (2002); (15) Milvang-Jensen et al. (2008); (16) Postman et al. (2001); (17) Rosati et al. (2009) and data provided by P. Rosati; (18) Tanaka et al. (2008); (19) Tran et al. (2007); (20) Vulcani et al. (2012); (21) White et al. (2005).

of the cluster center and the  $R_{200}$  radius<sup>2</sup> computed in Sect. 3, is listed here to show the radial extension of the original cluster data sample.

Our cluster sample results from a collection of data from several sources which results in different sampling criteria related to the strategy used by the different observers to select spectroscopic targets. As a result, the data samples we use differ in their

photometric properties and completeness limits. This is not expected to affect our results, which are based on kinematics and relative comparisons, but we suggest to be cautious in drawing other conclusions. For instance, we report the numbers of cluster galaxies only to stress the relative statistical weights of the different samples. Since these numbers are dependent on the different (and often poorly known) selection functions of the original data sources, they are not representative of the intrinsic relative fractions of the different cluster populations.

<sup>2</sup> The radius  $R_\delta$  is the radius of a sphere with mass overdensity  $\delta$  times the critical density at the redshift of the galaxy system. Correspondingly,  $M_{200}$  is the total mass contained within this radius.

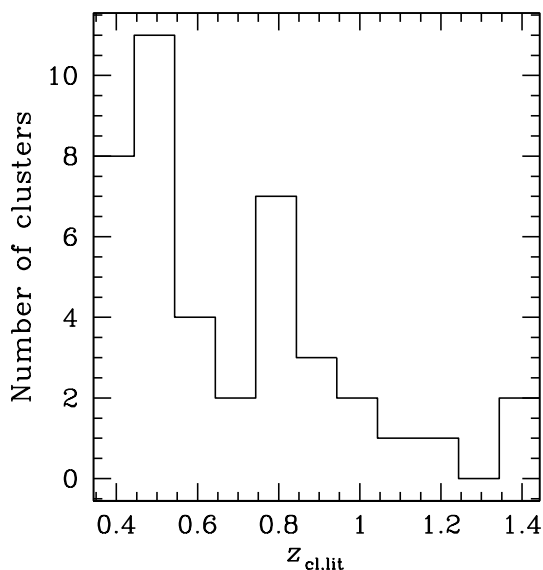


Fig. 1. Distribution of redshifts for the 41 clusters of the sample.

### 3. Member selection and global cluster properties

To select cluster members, we applied a two-step procedure introduced by Fadda et al. (1996) and called “peak+gap” (P+G) in more recent studies (Biviano et al. 2013; Girardi et al. 2015). The method is a combination of the 1D adaptive-kernel method DEDICA (Pisani 1993; see also the Appendix of Girardi et al. 1996) and the “shifting gapper” method, which uses both position and velocity information (Fadda et al. 1996). The 1D-DEDICA method is a non parametric, adaptive method of density reconstruction, optimized as described in Pisani (1993). It is used to detect the cluster peak in the redshift distribution and assign the respective galaxies. For each cluster, we detected a peak at the cluster redshift reported by the literature, that is with a difference  $\Delta z < 0.003$ , with high significant c.l. (i.e.  $\geq 99\%$ , with the exception of RX J1716.6+6708 at the 98% c.l.). In the few cases where secondary peaks are also detected, we considered as belonging to the cluster those peaks  $\leq 2500 \text{ km s}^{-1}$  apart from the main peak and having at least a  $\geq 25\%$  of overlapping with the main peak. For each cluster, the preliminary cluster members are used to compute the center as the mean position in R.A. and Dec. of the galaxies using the biweight estimator (ROSTAT software, Beers et al. 1990). The “shifting gapper” procedure rejects galaxies that are too far in velocity from the main body of galaxies and within a fixed radial bin that shifts along the distance from the cluster center. The procedure is iterated until the number of cluster members converges to the final value. Following Fadda et al. (1996) we used a gap of  $1000 \text{ km s}^{-1}$  – in the cluster rest-frame – and a bin of 0.6 Mpc, or large enough to include 15 galaxies.

For each cluster, we computed its global properties through a recursive procedure. First, we estimated the mean cluster redshift, using the biweight estimator, and the robust estimate of the LOS velocity dispersion. For robust estimate we mean that we used the biweight estimator and the gapper estimator for samples with  $\geq$  or  $< 15$  member galaxies, respectively, following the suggestions of Beers et al. (1990) and Girardi et al. (1993). In the computation of velocity dispersions we also applied the

cosmological correction and the standard correction for velocity errors (Danese et al. 1980). To obtain a first estimate of the radius  $R_{200}$  and the cluster mass  $M_{200}$  there contained, we used the theoretical relation between mass and velocity dispersion of Munari et al. (2013; Eq. 1), which those authors verified on simulated clusters. We considered the galaxies within this first estimate of  $R_{200}$  to recompute the galaxy properties and in particular the final estimate of  $R_{200}$  and  $M_{200}$ . Using galaxies within this fiducial estimate of  $R_{200}$ , we estimated the final cluster properties, that are the cluster center, the mean redshift  $z_{cl}$ , and the velocity dispersion  $\sigma_v$ , as listed in Table 2. We do not list the errors on  $R_{200}$  (resp.  $M_{200}$ ) since its relative error is nominally equal (resp. three times) that on  $\sigma_v$  considering the scaling relation,  $R_{200} \propto \sigma_v$  (resp.  $M_{200} \propto \sigma_v^3$ ). An additional  $\sim 10\%$  uncertainty on  $M_{200}$  arises from the intrinsic scatter between  $M_{200}$  and  $\sigma_v$ , as indicated by numerical simulations (Munari et al. 2013).

Note that, 23 clusters are not sampled out to  $R_{200}$  (see Table 1). We used the other 18 well sampled clusters to verify that this undersampling does not introduce any bias in our estimate of the velocity dispersion and, consequently, of  $R_{200}$  and  $M_{200}$ . For these 18 clusters, we compared the distribution of the velocity dispersions computed within  $0.5R_{200}$  and that within  $R_{200}$ . We obtained no significant evidence of difference according to the Kolmogorov-Smirnov test (hereafter KS-test; see, e.g., Lederman 1984), and according to two more sensitive tests, the Sign and Wilcoxon Signed-ranks tests (hereafter S- and W-tests, e.g., Siegel 1956).

### 4. Populations of red and blue galaxies

In order to separate red/passive from blue/star-forming galaxies, we used a color based procedure. As much as possible, we considered the two magnitude bands in such way that the Balmer break at the cluster redshift lies roughly between the two filters (see Fig. 18 of Westra et al. 2010). The color distribution is analyzed using the Kaye’s mixture model (KMM) method, as implemented by Ashman et al. (1994), to detect the color bimodality and define the respective group partition and, consequently, the value of the color cut (see Fig. 2 as an example).

The KMM procedure fails in detecting a significant bimodality in eight clusters, typically those having very few available data, and we used alternative procedures. In four clusters, to define the color cut, we adopted the intermediate value between the typical color of red and blue galaxies at  $z = 0$  (Fukugita et al. 1995), conveniently shifted at the cluster redshift using the k- and evolutionary corrections by Poggianti (1997). In the four distant clusters, for which the magnitude corrections are less reliable, we preferred to use spectroscopic features to separate red/passive from blue/star-forming galaxies. We defined as star-forming galaxies those with the [OII] emission line in their spectrum. When EW[OII] measures were available, we defined as star-forming galaxies those with  $\text{EW[OII]} \geq 15 \text{ \AA}$  (see, e.g., Postman et al. 1998; Hammer et al. 1997). For the eleven clusters where both good magnitude and spectroscopic information are available, the location of ELGs in the color-mag diagram supports the good agreement of the photometric- and spectroscopic-based methods (see Fig. 2 – left panel – for an example). For each cluster, Table 3 lists: the number of member galaxies with measured magnitudes,  $N_m$  (Col. 2); the color and magnitude used in our analysis (Cols. 3 and 4); the adopted color cut (Col. 5). In the case of the spectroscopic based separation,  $N_m$  refers to the number of galaxies with available EW[OII] information. The relevant information about the reference sources of magnitudes is listed in Table 1.

**Table 2.** Cluster properties.

Cluster name	$N_{\text{all}}$	$N_{R200}$	$\alpha$ (J2000) (hh:mm:ss)	$\delta$ (J2000) (° :′ :″)	$z_{\text{cl}}$	$\sigma_V$ (km s <sup>-1</sup> )	$R_{200}$ (Mpc)	$M_{200}$ (10 <sup>14</sup> M <sub>⊙</sub> )
MS 0015.9+1609	50	35	00:18:31.95	+16:25:19.6	0.5505±0.0005	916 <sup>+139</sup> <sub>-102</sub>	1.39	5.58
CL 0024+1652	100	99	00:26:33.82	+17:10:06.7	0.3936±0.0003	892 <sup>+56</sup> <sub>-91</sub>	1.55	6.37
RX J0152.7-1357	125	124	01:52:42.20	-13:57:54.5	0.8359±0.0004	1335 <sup>+65</sup> <sub>-63</sub>	1.78	16.42
MS 0302.5+1717	28	28	03:05:17.99	+17:28:30.0	0.4242±0.0004	666 <sup>+62</sup> <sub>-72</sub>	1.13	2.60
MS 0302.7+1658	34	33	03:05:31.68	+17:10:06.1	0.4248±0.0005	793 <sup>+120</sup> <sub>-87</sub>	1.35	4.39
CL 0303+1706	46	44	03:06:14.40	+17:18:00.3	0.4188±0.0004	804 <sup>+110</sup> <sub>-139</sub>	1.37	4.59
MS 0451.6-0305	44	44	04:54:10.96	-03:01:07.8	0.5401±0.0006	1242 <sup>+72</sup> <sub>-106</sub>	1.98	15.77
RDCS J0910+5422	23	16	09:10:45.70	+54:22:22.4	1.1004±0.0006	705 <sup>+153</sup> <sub>-139</sub>	0.81	2.08
CL 0939+4713	70	70	09:42:58.68	+46:58:59.9	0.4060±0.0005	1156 <sup>+96</sup> <sub>-86</sub>	1.99	13.76
CL J1018.8-1211	34	27	10:18:46.71	-12:12:23.1	0.4734±0.0004	532 <sup>+84</sup> <sub>-60</sub>	0.94	1.59
CL J1037.9-1243a	47	38	10:37:49.28	-12:45:12.0	0.4251±0.0003	521 <sup>+59</sup> <sub>-32</sub>	0.86	1.15
CL J1037.9-1243	19	17	10:37:53.15	-12:43:44.1	0.5785±0.0005	564 <sup>+248</sup> <sub>-180</sub>	0.88	1.44
CL J1040.7-1155	30	17	10:40:40.27	-11:56:12.6	0.7045±0.0004	517 <sup>+80</sup> <sub>-44</sub>	0.79	1.21
CL J1054.4-1146	49	33	10:54:25.59	-11:46:42.5	0.6981±0.0004	607 <sup>+120</sup> <sub>-83</sub>	0.85	1.53
CL J1054.7-1245	36	23	10:54:43.48	-12:46:23.8	0.7504±0.0004	525 <sup>+137</sup> <sub>-72</sub>	0.74	1.07
MS 1054.4-0321	143	140	10:57:00.47	-03:37:32.9	0.8307±0.0003	1113 <sup>+78</sup> <sub>-57</sub>	1.49	9.54
CL J1059.2-1253	42	39	10:59:08.61	-12:53:51.6	0.4564±0.0003	523 <sup>+60</sup> <sub>-49</sub>	0.87	1.24
CL J1103.7-1245a	17	10	11:03:35.99	-12:46:45.0	0.6261±0.0004	357 <sup>+48</sup> <sub>-189</sub>	0.60	0.50
CL J1103.7-1245	22	9	11:03:44.69	-12:45:34.1	0.9580±0.0006	448 <sup>+155</sup> <sub>-116</sub>	0.49	0.39
RX J1117.4+0743	37	37	11:17:26.24	+07:43:50.4	0.4857±0.0008	1426 <sup>+119</sup> <sub>-97</sub>	2.34	24.65
CL J1138.2-1133a	14	14	11:38:06.09	-11:36:15.1	0.4546±0.0005	510 <sup>+74</sup> <sub>-63</sub>	0.85	1.15
CL J1138.2-1133	49	48	11:38:09.86	-11:33:35.3	0.4797±0.0003	712 <sup>+65</sup> <sub>-86</sub>	1.17	3.08
CL J1216.8-1201	66	65	12:16:44.59	-12:01:20.3	0.7939±0.0004	1004 <sup>+79</sup> <sub>-68</sub>	1.37	7.16
RX J1226.9+3332	50	46	12:26:58.34	+33:32:52.6	0.8912±0.0005	1039 <sup>+116</sup> <sub>-107</sub>	1.34	7.49
XMMU J1230.3+1339	13	8	12:30:17.93	+13:39:03.8	0.9755±0.0007	548 <sup>+206</sup> <sub>-98</sub>	0.75	1.44
CL J1232.5-1250	54	54	12:32:30.76	-12:50:41.1	0.5418±0.0005	1089 <sup>+108</sup> <sub>-100</sub>	1.73	10.62
RDCS J1252-2927	38	28	12:52:54.40	-29:27:17.4	1.2367±0.0005	789 <sup>+96</sup> <sub>-89</sub>	0.85	2.85
CL J1301.7-1139a	17	17	13:01:36.74	-11:39:24.9	0.3969±0.0003	388 <sup>+74</sup> <sub>-64</sub>	0.67	0.52
CL J1301.7-1139	37	31	13:01:37.08	-11:39:33.0	0.4831±0.0004	704 <sup>+90</sup> <sub>-83</sub>	1.14	2.83
CL J1324+3011	44	42	13:24:48.68	+30:11:20.2	0.7548±0.0005	871 <sup>+139</sup> <sub>-97</sub>	1.20	4.54
CL J1353.0-1137	21	17	13:53:02.15	-11:37:10.9	0.5880±0.0005	615 <sup>+257</sup> <sub>-127</sub>	0.92	1.69
CL J1354.2-1230	23	14	13:54:10.16	-12:31:03.1	0.7593±0.0005	489 <sup>+88</sup> <sub>-45</sub>	0.74	1.07
CL J1411.1-1148	25	24	14:11:04.30	-11:48:10.1	0.5196±0.0005	784 <sup>+145</sup> <sub>-103</sub>	1.26	4.02
3C 295	25	25	14:11:20.06	+52:12:16.5	0.4593±0.0011	1677 <sup>+192</sup> <sub>-147</sub>	2.80	40.72
CL 1601+4253	55	53	16:03:09.84	+42:45:13.1	0.5401±0.0003	697 <sup>+82</sup> <sub>-84</sub>	1.11	2.79
CL J1604+4304	16	13	16:04:24.70	+43:04:48.2	0.8983±0.0007	683 <sup>+282</sup> <sub>-139</sub>	0.88	2.12
CL J1604+4321	37	35	16:04:34.41	+43:21:01.6	0.9220±0.0004	669 <sup>+231</sup> <sub>-119</sub>	0.91	2.42
MS 1621.5+2640	104	54	16:23:37.03	+26:35:08.7	0.4257±0.0003	757 <sup>+84</sup> <sub>-75</sub>	1.29	3.81
RX J1716.6+6708	31	28	17:16:48.86	+67:08:22.3	0.8063±0.0008	1299 <sup>+136</sup> <sub>-158</sub>	1.76	15.39
XMMXCS J2215.9-1738	41	27	22:15:58.75	-17:37:57.9	1.4569±0.0005	745 <sup>+120</sup> <sub>-86</sub>	0.70	2.01
XMMU J2235.3-2557	30	20	22:35:20.81	-25:57:22.0	1.3905±0.0007	910 <sup>+187</sup> <sub>-82</sub>	0.96	4.86

**Notes.** Column 1: cluster name; Col. 2: the number of all fiducial cluster members,  $N_{\text{all}}$ ; Col. 3: the number of member galaxies contained within  $R_{200}$ ,  $N_{R200}$ ; Cols. 4 and 5: the cluster center; Col. 6: the mean redshift,  $z_{\text{cl}}$ ; Col. 7: the LOS velocity dispersion,  $\sigma_V$ ; Cols. 8 and 9:  $R_{200}$  and  $M_{200}$ .

We considered the cluster regions within  $2R_{200}$ . Out to  $2R_{200}$  the cluster density and mass profiles are a reasonable extrapolation of those determined within  $R_{200}$  (Biviano & Girardi 2003). A requirement of our catalog is that each cluster is sampled at least with four red and four blue galaxy members within  $2R_{200}$ . Generally, the clusters in our catalog are much better sampled (see Cols. 2 and 4 in Table 4), with 20 red galaxies and 14 blue galaxies per cluster (median values). Table 4 lists the velocity dispersions of the red and blue galaxies within  $2R_{200}$ . The values of  $\sigma_{V,\text{red}}$  and  $\sigma_{V,\text{blue}}$  correlate at the > 99.99% c.l. according to the Spearman test (coefficient value of 0.70, see Fig. 3).

## 5. Analysis and results

### 5.1. Galaxy color segregation in velocity space

To investigate the relative kinematics of red and blue galaxy populations, we applied a set of tests. As for the individual clusters, we checked for different values of velocity dispersions of the two galaxy populations by applying the standard F-test (Press et al. 1992). We found that only 6 (9) of the 41 clusters show evidence of a kinematical difference at the 95% (90%) c.l.. In most of these cases, that is 5 (7) clusters, we found  $\sigma_{V,\text{blue}} > \sigma_{V,\text{red}}$  (see Table 5).

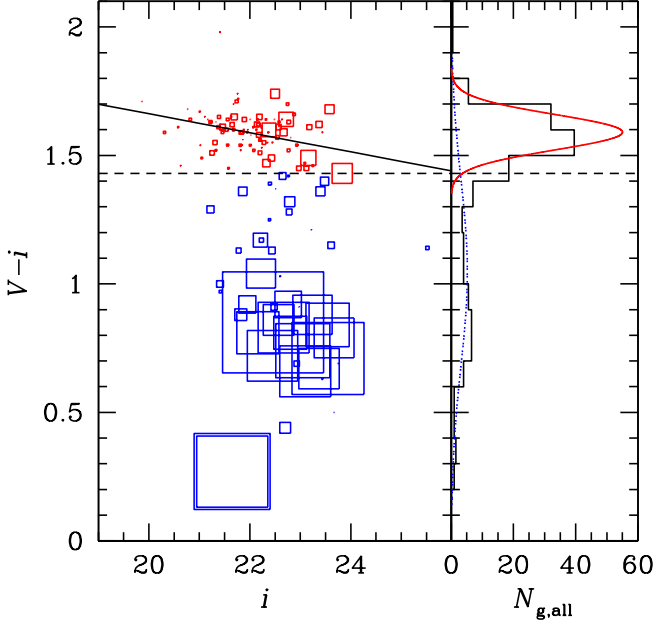


**Fig. 2.** Separation between red and blue galaxies in the MS 1054.4–0321 cluster. *Left panel:* color-magnitude diagram. The horizontal dashed line indicates the color cut as obtained using the  $V - i$  colors for member galaxies. For this well sampled cluster we also show the red sequence line as fitted with a two sigma procedure applied to the red galaxies (black solid line). Larger sizes of the symbols for larger EW[OII] show the good agreement between the photometric and spectroscopic methods to separate red/passive from blue/star-forming galaxy populations. *Right panel:* distribution of  $V - i$  colors for member galaxies. The two Gaussians are obtained through the KMM method and allow us to define the color cut in the left panel.

We compared the  $\sigma_{V,\text{red}}$  distribution and the  $\sigma_{V,\text{blue}}$  distribution. According to the KS-test, the probability that the two distributions are drawn from the same parent distribution is  $\sim 24\%$ , i.e. there is no evidence of a significant difference. The cumulative distributions are compared in Fig. 4 and the separation between the two distribution median values is  $75 \text{ km s}^{-1}$ , that is  $\sim 11\%$  of the median value of global  $\sigma_V$ . The availability of two measures,  $\sigma_{V,\text{red}}$  and  $\sigma_{V,\text{blue}}$ , for each cluster, allows us to also apply the S- and W-tests, which are more sensitive tests than the KS-test, and to look for a possible systematic, even if small difference. According to the S- and W-tests,  $\sigma_{V,\text{blue}}$  is larger than  $\sigma_{V,\text{red}}$  at the 97.02% and 99.45% c.l.s., respectively. Out of 41 clusters, the number of those with  $\sigma_{V,\text{blue}} > \sigma_{V,\text{red}}$  is 27 (see inset in Fig. 3).

As a final test, we considered the projected phase space, that is the rest-frame velocities  $V_{\text{rf}} = (V - \langle V \rangle) / (1 + z)$  vs clustercentric distance  $R$ , of two ensemble clusters, one for red and one for blue galaxies. These two ensemble cluster data are obtained by stacking all together the red (or blue) galaxies of each cluster normalizing the velocity and the clustercentric distance of each galaxy with the  $\sigma_V$  and  $R_{200}$  values of the parent cluster. The result is shown in Fig. 5 (upper panel), where we also trace the limits due to the escape velocity in the cluster, assuming a typical cluster mass distribution described by a NFW density profile with a concentration parameter  $c=3.8$ , which is typical for halos of mass  $M = 3 \times 10^{14} M_{\odot}$  at  $z = 0.6$ , the median values in our sample (Dolag et al. 2004). The "trumpet shape" of the projected phase space data distribution and the good agreement with the

**Table 3.** Color cuts to separate blue from red galaxies.

Cluster name	$N_m$	Color	Mag	Cut
MS 0015.9+1609	50	$g - r$	$r$	1.20
CL 0024+1652	78	$g - r$	$r$	1.20
RX J0152.7–1357	106	$r - K_s$	$K_s$	2.52
MS 0302.5+1717	28	$R - I$	$I$	0.76
MS 0302.7+1658 <sup>a</sup>	34	$g - r$	$r$	1.26
CL 0303+1706	37	$g - r$	$r$	1.37
MS 0451.6–0305	44	$g' - r'$	$r'$	1.76
RDCS J0910+5422	23	$i - z$	$z$	0.82
CL 0939+4713	48	$g - r$	$r$	1.13
CL J1018.8–1211	34	$B - I$	$I$	2.94
CL J1037.9–1243a	47	$V - I$	$I$	1.60
CL J1037.9–1243	19	$V - R$	$R$	1.08
CL J1040.7–1155	30	$R - I$	$I$	1.02
CL J1054.4–1146	49	$R - I$	$I$	2.15
CL J1054.7–1245	35	$R - I$	$I$	1.11
MS 1054.4–0321	142	$V - i$	$i$	1.43
CL J1059.2–1253	41	$B - I$	$I$	3.20
CL J1103.7–1245a <sup>a</sup>	15	$V - I$	$I$	2.20
CL J1103.7–1245	22	$R - I$	$I$	1.20
RX J1117.4+0743 <sup>a</sup>	37	$g' - r'$	$r'$	1.78
CL J1138.2–1133a	14	$V - I$	$I$	1.88
CL J1138.2–1133	49	$V - I$	$I$	1.69
CL J1216.8–1201	66	$R - I$	$I$	1.28
RX J1226.9+3332	50	$i' - z'$	$z'$	0.63
XMMU J1230.3+1339	13	$i - z$	$z$	0.37
CL J1232.5–1250	54	$B - I$	$I$	3.78
RDCS J1252–2927 <sup>b</sup>	38	–	–	–
CL J1301.7–1139a	17	$B - I$	$I$	3.02
CL J1301.7–1139	37	$B - I$	$I$	3.20
CL J1324+3011	44	$R - I$	$I$	1.21
CL J1353.0–1137	21	$V - I$	$I$	2.16
CL J1354.2–1230	22	$V - I$	$I$	2.11
CL J1411.1–1148	25	$B - I$	$I$	3.58
3C 295 <sup>a</sup>	25	$g - r$	$r$	1.40
CL 1601+4253	50	$g - r$	$r$	1.20
CL J1604+4304	15	$B - R$	$R$	1.05
CL J1604+4321	37	$B - R$	$R$	2.00
MS 1621.5+2640	104	$g - r$	$r$	1.27
RX J1716.6+6708 <sup>b</sup>	31	–	–	–
XMMXCS J2215.9–1738 <sup>b</sup>	41	–	–	–
XMMU J2235.3–2557 <sup>b</sup>	29	–	–	–

**Notes.** <sup>(a)</sup> Color cut based on the typical color of galaxies (Fukugita et al. 1995); <sup>(b)</sup> Selection based on the EW[OII] information.

escape velocity curves should be considered as a posteriori sanity check of the member selection procedure, which we made completely model-independent. In principle, the projection of possible non-member galaxies, likely blue field galaxies, onto the "trumpet shape" cannot be excluded. However, according to the analysis of N-body cosmological simulations (Biviano et al. 2006), their effect should be that of slightly decreasing the value of the velocity dispersion, that is an opposite effect with respect to the segregation effect reported in the present and previous studies.

**Table 4.** Velocity dispersions of red and blue populations.

Cluster name	$N_r$	$\sigma_{V,\text{red}}$ (km s <sup>-1</sup> )	$N_b$	$\sigma_{V,\text{blue}}$ (km s <sup>-1</sup> )
MS 0015.9+1609	39	994 <sup>+138</sup> <sub>-87</sub>	11	809 <sup>+538</sup> <sub>-140</sub>
CL 0024+1652	49	1042 <sup>+115</sup> <sub>-110</sub>	29	889 <sup>+108</sup> <sub>-116</sub>
RX J0152.7-1357	91	1270 <sup>+85</sup> <sub>-68</sub>	15	1750 <sup>+396</sup> <sub>-289</sub>
MS 0302.5+1717	24	638 <sup>+63</sup> <sub>-82</sub>	4	900 <sup>+482</sup> <sub>-420</sub>
MS 0302.7+1658	24	669 <sup>+166</sup> <sub>-113</sub>	10	906 <sup>+623</sup> <sub>-282</sub>
CL 0303+1706	21	690 <sup>+309</sup> <sub>-320</sub>	16	284 <sup>+132</sup> <sub>-150</sub>
MS 0451.6-0305	28	1269 <sup>+124</sup> <sub>-102</sub>	16	1115 <sup>+161</sup> <sub>-169</sub>
RDCS J0910+5422	16	721 <sup>+153</sup> <sub>-131</sub>	6	768 <sup>+267</sup> <sub>-252</sub>
CL 0939+4713	34	1212 <sup>+147</sup> <sub>-117</sub>	14	996 <sup>+207</sup> <sub>-156</sub>
CL J1018.8-1211	19	449 <sup>+85</sup> <sub>-54</sub>	15	493 <sup>+180</sup> <sub>-85</sub>
CL J1037.9-1243a	26	555 <sup>+133</sup> <sub>-63</sub>	21	560 <sup>+76</sup> <sub>-54</sub>
CL J1037.9-1243	6	347 <sup>+113</sup> <sub>-72</sub>	13	594 <sup>+231</sup> <sub>-274</sub>
CL J1040.7-1155	12	383 <sup>+89</sup> <sub>-45</sub>	18	450 <sup>+82</sup> <sub>-59</sub>
CL J1054.4-1146	28	447 <sup>+114</sup> <sub>-75</sub>	21	715 <sup>+112</sup> <sub>-67</sub>
CL J1054.7-1245	23	545 <sup>+130</sup> <sub>-76</sub>	11	476 <sup>+286</sup> <sub>-105</sub>
MS 1054.4-0321	96	1050 <sup>+76</sup> <sub>-74</sub>	46	1268 <sup>+203</sup> <sub>-148</sub>
CL J1059.2-1253	22	401 <sup>+71</sup> <sub>-54</sub>	19	613 <sup>+81</sup> <sub>-75</sub>
CL J1103.7-1245a	7	341 <sup>+163</sup> <sub>-97</sub>	7	371 <sup>+82</sup> <sub>-187</sub>
CL J1103.7-1245	5	571 <sup>+273</sup> <sub>-162</sub>	9	227 <sup>+100</sup> <sub>-36</sub>
RX J1117.4+0743	19	1066 <sup>+441</sup> <sub>-227</sub>	18	1654 <sup>+248</sup> <sub>-156</sub>
CL J1138.2-1133a	7	418 <sup>+131</sup> <sub>-50</sub>	7	486 <sup>+657</sup> <sub>-57</sub>
CL J1138.2-1133	20	484 <sup>+123</sup> <sub>-79</sub>	29	867 <sup>+133</sup> <sub>-40</sub>
CL J1216.8-1201	35	976 <sup>+122</sup> <sub>-78</sub>	31	959 <sup>+117</sup> <sub>-71</sub>
RX J1226.9+3332	43	926 <sup>+127</sup> <sub>-101</sub>	7	1199 <sup>+698</sup> <sub>-258</sub>
XMMU J1230.3+1339	8	768 <sup>+192</sup> <sub>-71</sub>	5	605 <sup>+279</sup> <sub>-60</sub>
CL J1232.5-1250	26	1025 <sup>+235</sup> <sub>-91</sub>	28	1062 <sup>+147</sup> <sub>-129</sub>
RDCS J1252-2927	21	787 <sup>+110</sup> <sub>-108</sub>	16	775 <sup>+143</sup> <sub>-92</sub>
CL J1301.7-1139a	12	331 <sup>+89</sup> <sub>-52</sub>	5	586 <sup>+176</sup> <sub>-193</sub>
CL J1301.7-1139	20	543 <sup>+187</sup> <sub>-81</sub>	17	778 <sup>+143</sup> <sub>-65</sub>
CL J1324+3011	25	723 <sup>+128</sup> <sub>-102</sub>	19	1028 <sup>+248</sup> <sub>-203</sub>
CL J1353.0-1137	8	277 <sup>+62</sup> <sub>-19</sub>	13	810 <sup>+182</sup> <sub>-96</sub>
CL J1354.2-1230	11	455 <sup>+91</sup> <sub>-63</sub>	10	446 <sup>+220</sup> <sub>-103</sub>
CL J1411.1-1148	14	665 <sup>+112</sup> <sub>-73</sub>	11	741 <sup>+264</sup> <sub>-135</sub>
3C 295	12	1354 <sup>+168</sup> <sub>-228</sub>	13	1686 <sup>+310</sup> <sub>-190</sub>
CL 1601+4253	41	727 <sup>+108</sup> <sub>-97</sub>	9	764 <sup>+169</sup> <sub>-107</sub>
CL J1604+4304	10	500 <sup>+110</sup> <sub>-125</sub>	5	1158 <sup>+339</sup> <sub>-84</sub>
CL J1604+4321	11	591 <sup>+188</sup> <sub>-162</sub>	26	722 <sup>+289</sup> <sub>-144</sub>
MS 1621.5+2640	63	731 <sup>+80</sup> <sub>-68</sub>	34	780 <sup>+83</sup> <sub>-51</sub>
RX J1716.6+6708	18	1288 <sup>+237</sup> <sub>-166</sub>	13	1261 <sup>+162</sup> <sub>-454</sub>
XMMXCS J2215.9-1738	12	713 <sup>+156</sup> <sub>-215</sub>	24	647 <sup>+110</sup> <sub>-82</sub>
XMMU J2235.3-2557	17	851 <sup>+218</sup> <sub>-103</sub>	10	698 <sup>+148</sup> <sub>-98</sub>

The respective VDPs for red and blue galaxies are shown in the lower panel of Fig. 5. The VDPs are shown to decline, as expected, at least out to  $\geq R_{200}$ . In the outer regions, the uncertainties are very large and the fraction of possible interlopers, that is galaxies outside the theoretical escape velocity curves, survived to our member selection procedure, increases (see the upper panel of Fig. 5). Within  $R_{200}$  the VDP of blue galaxies is higher than that of red galaxies and the difference is significant at the  $> 99.99\%$  c.l. according to the  $\chi^2$ -test applied to the values of the four bins, which combine a total of 936 red and 532 blue galaxies. Table 6 summarizes the results of all the tests we applied.

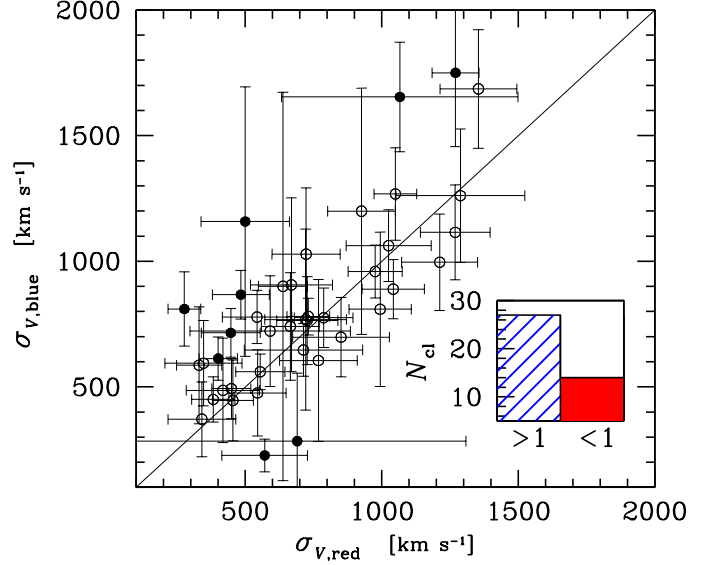


**Fig. 3.** Velocity dispersion of the red galaxy population vs velocity dispersion of the blue galaxy population for all clusters of our sample. The filled symbols highlight the clusters where the two values are different according to the F-test (at a c.l.  $\geq 90\%$ , see Table 5). Inset shows the number of clusters with  $\sigma_{V,\text{blue}}/\sigma_{V,\text{red}} > 1$  (blue shaded bar) and the number of clusters with  $\sigma_{V,\text{blue}}/\sigma_{V,\text{red}} < 1$  (red solid bar).

**Table 5.** Clusters where  $\sigma_{V,\text{red}} \neq \sigma_{V,\text{blue}}$ .

Cluster name	F-test Prob <sub>#</sub>
RX J0152.7-1357	93%
CL 0303+1706 <sup>a</sup>	99.9%
CL J1054.4-1146	98%
CL J1059.2-1253	94%
CL J1103.7-1245 <sup>a</sup>	97%
RX J1117.4+0743	93%
CL J1138.2-1133	99%
CL J1353.0-1137	99%
CL J1604+4304	97%

**Notes.** <sup>(a)</sup> Cases with  $\sigma_{V,\text{red}} > \sigma_{V,\text{blue}}$ . In other cases  $\sigma_{V,\text{blue}} > \sigma_{V,\text{red}}$ .

To investigate the variation of the kinematical difference between red and blue galaxy populations at different redshifts, we divided the cluster sample in three subsamples, Low- $z$  sample with  $z < 0.5$ , Medium- $z$  with  $0.5 \leq z < 0.8$ , High- $z$  with  $z \geq 0.8$ , having a roughly comparable number of clusters and galaxies. We applied the above-described set of tests to the three subsamples. Fig. 6 points out the relation between  $\sigma_{V,\text{blue}}$  and  $\sigma_{V,\text{red}}$  separately for the three subsamples and shows that clusters of the High- $z$  sample are equally split by  $\sigma_{V,\text{blue}} > \sigma_{V,\text{red}}$  and  $\sigma_{V,\text{blue}} < \sigma_{V,\text{red}}$  values. Fig. 7 shows the variation of the normalized  $\sigma_{V,\text{blue}}$  (and  $\sigma_{V,\text{red}}$ ) values with redshift, no difference is found for the High- $z$  sample. To apply the VDP  $\chi^2$ -test, we considered data binned in three intervals within  $1.2R_{200}$  (see Fig. 8) for a total of 349 red and 224 blue galaxies in the Low- $z$  sample,



**Table 6.** Statistical results about the relative kinematics of red and blue populations.

Sample	$z$ range	$N_{\text{cl}}$	$N_{\text{g}}$	$N_{\text{cl,F}}$	$\Delta\sigma_V$ ( $\text{km s}^{-1}$ )	$\Delta\sigma_V/\sigma_V$	$N_{\text{cl,b>r}}$	S-test Prob $_{\neq}$	W-test Prob $_{\neq}$	VDP $\chi^2$ -test Prob $_{\neq}$
Whole	$0.4 \leq z \leq 1.5$	41	1674	5 (7)	75	11%	27	97%	99%	>99.99%
Low-z	$0.4 \leq z < 0.5$	15	623	2 (4)	170	24%	12	98%	98%	99%
Medium-z	$0.5 \leq z < 0.8$	13	455	2 (2)	148	14%	9	87%	93%	98%
High-z	$0.8 \leq z \leq 1.5$	13	596	1 (1)	48	6%	6	50%	73%	96%

**Notes.** Column 1: sample name; Col. 2: the redshift range of the sample; Col. 3: the number of clusters,  $N_{\text{cl}}$ ; Col. 4: the number of galaxies in the sample,  $N_{\text{g}}$ ; Col. 5: the number of clusters with  $\sigma_{V,\text{blue}} > \sigma_{V,\text{red}}$ , with a 95% (90%) c.l. significant difference according to the F-test,  $N_{\text{cl,F}}$ ; Col. 6: the difference between the median values of the  $\sigma_V$  distributions of red and blue galaxies,  $\Delta\sigma_V$ ; Col. 7: the same, but normalized to the median value of  $\sigma_V$  as computed using all galaxies,  $\Delta\sigma_V/\sigma_V$ ; Col. 8: the number of clusters with  $\sigma_{V,\text{blue}} > \sigma_{V,\text{red}}$ ,  $N_{\text{cl,b>r}}$ ; Cols. 9 and 10: the probability of difference according to the S- and W-tests; Col. 11: the probability of difference according to the  $\chi^2$ -test applied to the VDPs of the ensemble cluster. The results of the KS-test applied to the velocity dispersion distributions of red and blue galaxies are not listed since no evidence of significant difference is detected.

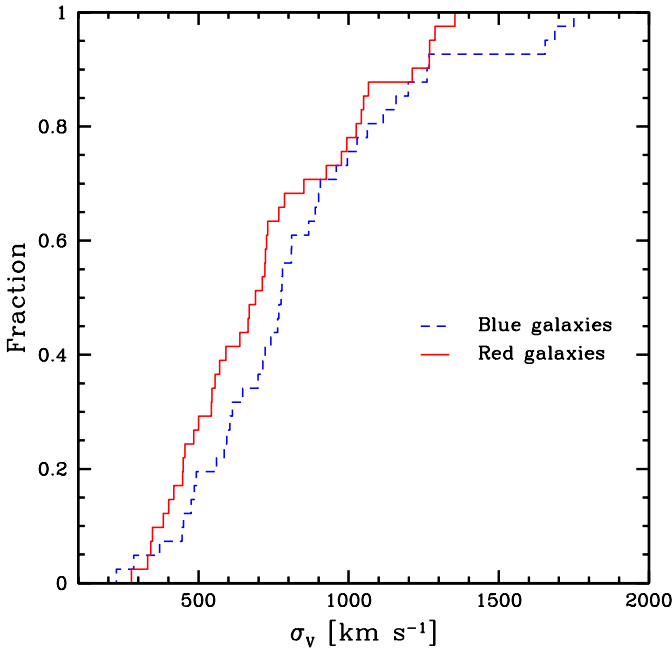


**Fig. 4.** Cumulative distributions of the velocity dispersions of red and blue galaxies.

247 red and 160 blue galaxies in the Medium- $z$  sample, 369 red and 193 blue galaxies in the High- $z$  sample. The results of the whole set of tests are listed in Table 6. We find that in the High- $z$  sample there is no or poorer evidence of kinematical segregation with respect to the other two samples, in particular with respect to the Low- $z$  sample.

## 5.2. Galaxy luminosity segregation in velocity space

As in previous studies of VLS, our analysis is based on the ensemble cluster. We restricted our analysis to galaxies within  $R_{200}$ . Because of the non homogeneity of the photometric data among different clusters in our sample, we adopted the same approach of Biviano et al. (1992) and normalized the magnitude of each galaxy with the magnitude of the third brightest galaxy ( $m_3$ ). We used one of the magnitude bands listed in Table 1 preferring red or NIR bands. We analyzed the behavior of  $|V_{\text{rf}}|$  vs  $m - m_3$

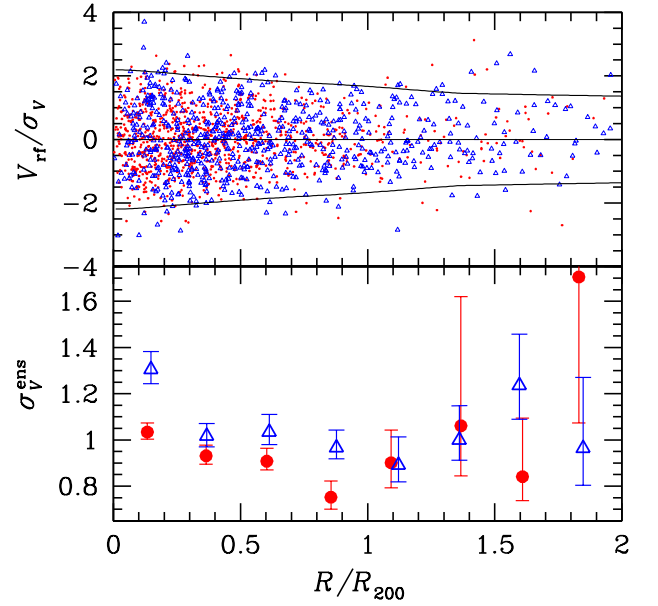


**Fig. 5.** *Upper panel:* rest-frame LOS velocity vs. projected cluster-centric distance for the galaxies of the ensemble cluster. Small red dots indicate red galaxies and blue triangles indicate blue galaxies. Black curves show the limits due to the escape velocity assuming a NFW mass profile (see text). *Lower panel:* velocity dispersion profiles (VDPs) for red and blue galaxies of the ensemble cluster (solid red circles and blue open triangles). Data are binned in intervals of 0.25 Mpc in the  $0-2R_{200}$  range. The point abscissae are set to the averages of the  $R/R_{200}$  values of each sample within the bins. The error bars are determined via a bootstrap resampling procedure.

and Figure 9 highlights the main results: i) the red galaxies have lower  $|V_{\text{rf}}|$  with respect to the blue galaxies, independent of their magnitudes; ii) both red and blue galaxies show evidence of velocity segregation. To statistically evaluate VLS, we also considered the correlation between  $|V_{\text{rf}}|/\sigma_V$  and  $m - m_3$  for galaxies having  $m - m_3 \leq 0.5$  or  $m - m_3 > 0.5$ , where  $m - m_3 = 0.5$  mag is the threshold value suggested by the inspection of Fig. 9. For the red (blue) galaxies with  $m - m_3 \leq 0.5$  we find that  $|V_{\text{rf}}|$  and  $m - m_3$  correlate at the  $\sim 94\%$  c.l. ( $\sim 90\%$ ) according to the Spearman



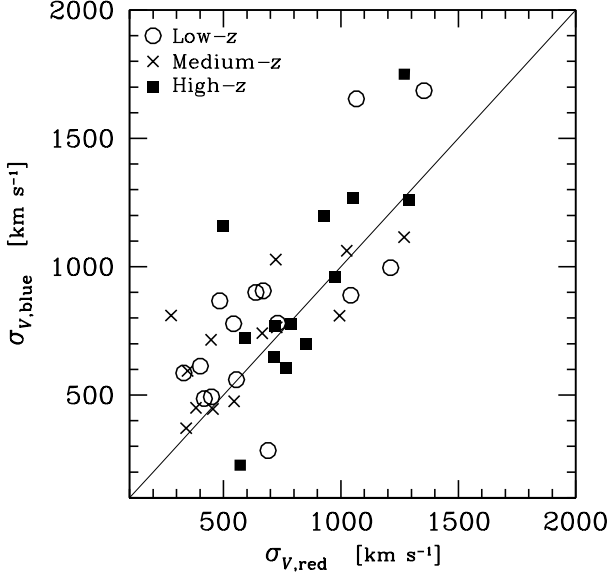


**Fig. 6.** Velocity dispersion of the blue galaxy population vs velocity dispersion of the red galaxy population for the three subsamples: Low- $z$  (open circles), Medium- $z$  (crosses), and High- $z$  (solid squares).

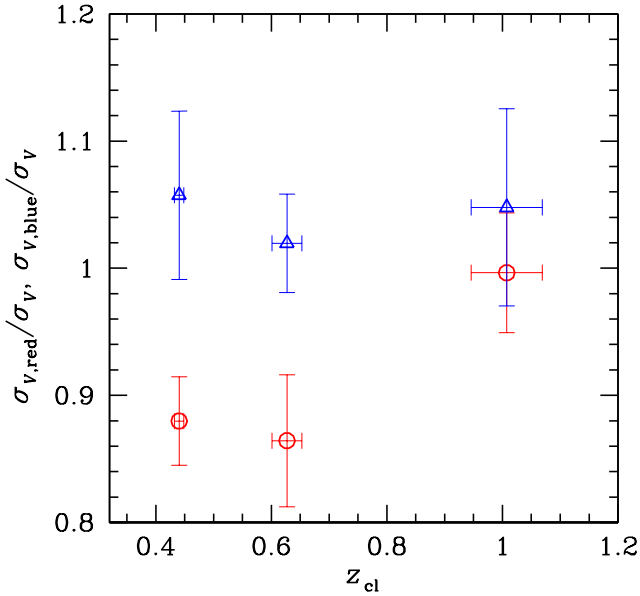


**Fig. 7.** Normalized velocity dispersion of the red galaxy population vs normalized velocity dispersion of the blue galaxy population for the three subsamples: Low- $z$ , Medium- $z$  and High- $z$ .

test. No significant correlation is found for red and blue galaxies with  $m - m_3 > 0.5$ .

To investigate a possible dependence of VLS with redshift, we also show the results for the three redshift subsamples. Although current data are not sufficient to obtain firm conclusions, the visual inspection of Fig. 10 suggests that the threshold value of segregation in the Low- $z$  sample lies at brighter magnitudes than the values in the Medium- $z$  and High- $z$  samples.

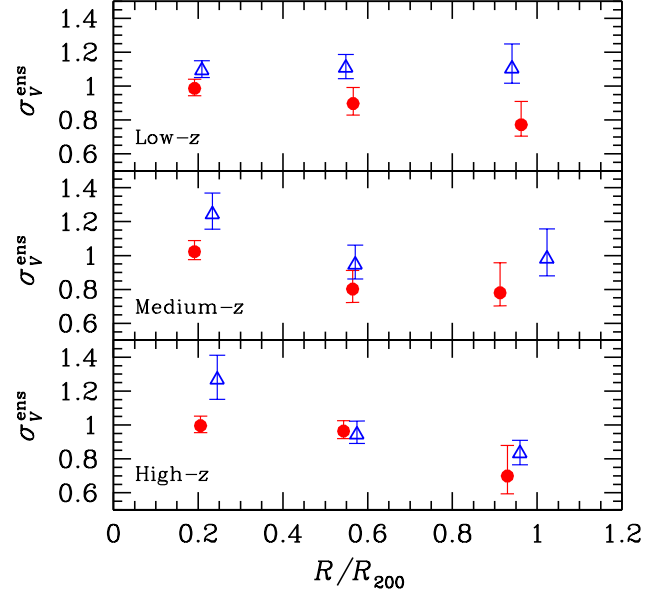


**Fig. 8.** Same as in Fig. 5, but for the ensemble clusters of the Low- $z$ , Medium- $z$ , and High- $z$  subsamples (*top*, *medium*, and *bottom* panels). Data are binned in intervals of 0.4 Mpc in the  $0-1.2R_{200}$  range.

## 6. Discussion

We find evidence of VCS in our sample of clusters. In our analysis, VCS is detected over the whole sampled galaxy luminosity range (see Fig 9). In particular, analyzing the clusters in three redshift ranges separately, Table 6 shows that the amount of VCS decreases with increasing redshift and that very poor or no evidence of segregation is found in the High- $z$  sample. Qualitatively, this is in agreement with the results of Biviano & Poggianti (2009) in EDisCS clusters at  $z \sim 0.4-0.8$  (our Low- $z$ +Medium- $z$  samples), for which there is much less evidence of VCS when compared to local clusters. Crawford et al. (2014) found no evidence of VCS between red sequence and blue cloud galaxies in five distant cluster ( $0.5 < z < 0.9$ ), but they did not analyze a local sample for comparison.

We confirm that the effect of VCS is quantitatively small and, therefore, difficult to detect. For instance, according to the KS-test, the  $\sigma_v$  distributions of red and blue galaxies might derive from the same parent distribution. We had to resort to very sensitive tests such as the S- and W-tests to detect a significant difference in the  $\sigma_v$  distributions. Indeed, as most previous positive detections in the literature, our most significant detection is obtained stacking galaxies of all clusters. Quantitatively, the estimates of the difference in  $\sigma_v$  reported in the literature are of the order of 10-20%, 30% at most (Biviano et al. 1997; Carlberg et al. 1997; Adami et al. 1998; de Theije & Katgert 1999; Haines et al. 2015) and vary according to the selection of the two populations. In fact, when the population is selected according to higher values of star formation rate, its  $\sigma_v$  is higher (Haines et al. 2015). The values we obtained in our study are comparable with those reported in the literature. We estimated that  $\sigma_v$  of red and blue galaxies differ for  $\Delta\sigma_v/\sigma_v \sim 20\%$  and  $10\%$  in the Low- $z$  and Medium- $z$  samples, and the median value of the ratios of the VDP binned values for blue and red galaxies is 1.2 (within  $R_{200}$ , see Fig. 5).

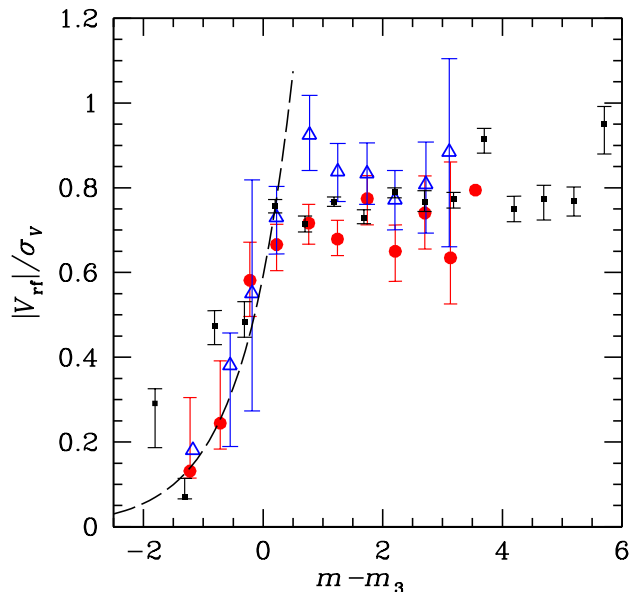


**Fig. 9.** Normalized velocities of red and blue galaxies (solid red circles and blue open triangles) vs  $m - m_3$ , where  $m_3$  is the magnitude of the third brightest galaxy in each cluster. Data are binned in intervals of 0.5 mag. The error bars are obtained via a bootstrap resampling procedure. Points without error bars indicate the values based on only three galaxies. The dashed line represents our fit for red galaxies in the  $m - m_3 \leq 0.5$  region. The results of Biviano et al. (1992) are shown for comparison (small black squares).

Taking into account the difficulties related to the detection and measure of VCS, any result is more reliable when obtained through an homogeneous analysis rather than comparing results from different authors. In this context, it is interesting that our results are in line with that of Biviano & Poggianti (2009) on a decreasing amount of VCS at higher redshifts, although their claim holds for clusters at  $z \sim 0.4$ – $0.8$ , while ours for clusters in the  $0.8 \leq z \leq 1.5$  range. The poor evidence of VCS in high redshift clusters can be explained in a scenario where the segregation develops as the result of a continuous, regular smooth accretion of field blue galaxies, then possibly evolving in red galaxies, into the cluster. VCS is erased when cluster-cluster mergers drive violent relaxation, and the frequency of such mergers is expected to be higher at higher redshift.

Since our cluster sample spans a large range of masses, of about two orders of magnitudes (see Table 2) we also checked for a possible dependence of VCS with mass. We find no significant correlation of  $\sigma_{V, \text{blue}}/\sigma_{V, \text{red}}$  vs the cluster mass. This agrees with the fact that the evidence of VCS, which is well known in clusters, is detected also in groups (Girardi et al. 2003; Ribeiro et al. 2010).

To our knowledge, this is the first study where VLS is detected in non local clusters. The  $|V_{\text{rf}}|$  vs  $m - m_3$  relation here detected is similar to that originally shown by Biviano et al. (1992). Assuming the mass-follows-light hypothesis, the faint galaxies can be described by a regime of velocity equipartition, while the bright galaxies can be better described by a regime of energy equipartition, with more massive objects being slower. Since we used red or NIR magnitude bands, the luminosity is a good indicator of the stellar mass, but the mass-follows-light assumption is needed to extrapolate our interpretation to the

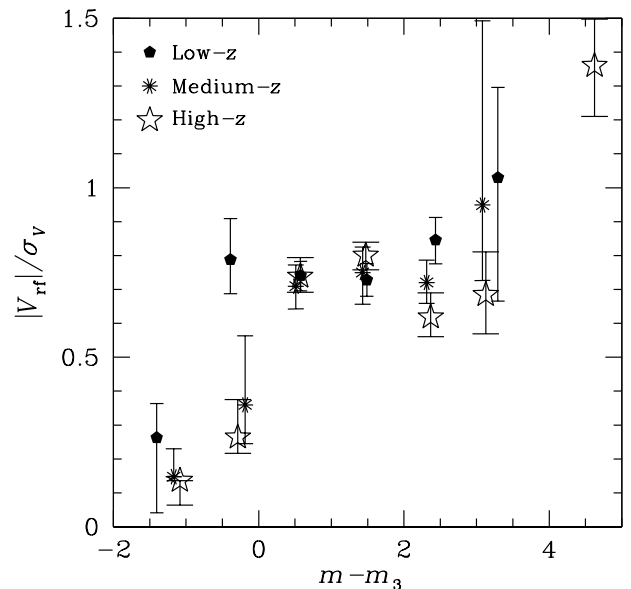


**Fig. 10.** Same as in Fig. 9 but for all red+blue galaxies and analyzing Low- $z$ , Medium- $z$ , and High- $z$  subsamples separately (polygons, asterisks, and stars, resp.)

whole, halo galaxy mass. As already discussed by other authors (Biviano et al. 1992; Mahajan et al. 2011) the most likely cause for the observed VLS is the dynamical friction process, whose characteristic time-scale is inversely proportional to mass.

We confirm that VLS holds for red galaxies and find for the first time evidence that the same segregation also applies to the population of blue galaxies. In fact, both Adami et al. (1998) and Ribeiro et al. (2013) found VLS for ellipticals/passive galaxies, but no (or even opposite) effect is reported for galaxies of other types. However, the inspection of Fig. 2b of Adami et al. (1998) suggests that their non detection might be rather due to the large uncertainties involved. The presence of the VLS for blue galaxies indicates that the kinematical relaxation time-scale is shorter than the transformation time-scale or that massive blue galaxies are robust against environmental effects and possible transformation to S0 (e.g., Moore et al. 1996; Bekki & Couch 2011).

A more detailed comparison of our results with those of Biviano et al. (1992, see also our Fig. 9) shows two differences. As a first difference, our  $|V_{\text{rf}}|$  and  $m - m_3$  relation is steeper than their relation. The fit of the logarithm of  $|V_{\text{rf}}|$  vs  $m - m_3$  gives a slope of  $0.52 \pm 0.05$  for red galaxies only, and  $0.48 \pm 0.04$  for all galaxies. For comparison, Biviano et al. (1992) obtained a value of 0.2, which is that expected in the case of energy equipartition (assuming a constant mass-to-light ratio). Adami et al. (1998) also claim that a 0.2 slope is consistent with their results, but large uncertainties are shown in their Fig. 1a and the inspection of their Fig. 2a for ellipticals rather suggests a steeper slope. The second difference concerns the threshold value between the two kinematic regimes. Biviano et al. (1992) indicate a threshold value around  $m_3$  and Adami et al. (1998) report that VLS concerns about four galaxies per cluster. In the whole sample, our results rather suggest  $m_3 + 0.5$  (Fig. 9) and we found that VLS concerns seven galaxies per cluster, computed as the median value of the numbers of galaxies with  $m - m_3 \leq 0.5$  in each cluster. However, both Biviano et al. (1992) and Adami et al. (1998) analyze local

clusters and the inspection of Fig. 10 indicates that the threshold value of VLS in the Low- $z$  sample lies at brighter magnitudes than the values in the Medium- $z$  and High- $z$  samples. Present data do not allow a precise quantitative conclusion, but suggest that the dependence of the segregation threshold should be taken into account. In particular, the possible explanation for a fainter threshold at higher redshifts might be that clusters at higher redshift have higher density. Per given galaxy mass, the greater the density of the surrounding medium, the stronger the effect of dynamical friction.

## 7. Summary and conclusions

In this study we present our results about color and luminosity segregation in velocity space (VCS and VLS, resp.) for a sample of 41 clusters at intermediate and high redshifts ( $0.4 \lesssim z \lesssim 1.5$ ), for a total of 4172 galaxies. The data have been taken from different sources in the literature, with the constraint that data for each single cluster come from one single source. Moreover, we applied homogeneous preliminary procedures to select cluster members, compute global cluster properties, in particular the LOS velocity dispersions  $\sigma_V$ , and separate blue from red galaxies. We restricted our analysis to the 1674 member galaxies within  $2R_{200}$  with photometric or spectroscopic information, 1023 red and 651 blue galaxies. We applied a set of different tests to study VCS and VLS. We used both the estimates of velocity dispersion for each individual cluster and the properties of an ensemble cluster obtained by stacking together galaxies of many clusters.

The main results of our analysis are summarized as follows.

- From the analysis of the whole sample we detect evidence of VCS according to several tests (S-, W-, and VDP  $\chi^2$ -tests), with the blue galaxy population having a larger  $\sigma_V$  than the red galaxy population.
- When analyzing three subsamples at different redshifts (Low- $z$  with  $z < 0.5$ , Medium- $z$  with  $0.5 \leq z < 0.8$ , High- $z$  with  $z \geq 0.8$ ), very poor or no evidence of VCS is found in the High- $z$  sample. The fact that VCS is weaker at higher redshifts has been already pointed out by Biviano & Poggianti (2009), although our threshold of no detection is at higher  $z$  than theirs. The disappearance of the VCS for distant clusters can be explained when considering that our High- $z$  sample is very close to the epoch of cluster formation, with major mergers driving violent relaxation which leads to the velocity equipartition regime.
- In agreement with previous studies we confirm that the effect of VCS is quantitatively small (10-20% in the  $\sigma_V$  estimate) and requires sensitive tests or the VDP analysis based on many galaxies. We conclude that VCS is an elusive effect, that might partly explains the discrepant claims reported in the literature on this issue.
- VCS concerns the whole magnitude range that we covered,  $\sim 4$  magnitudes down to  $m_3$ ; more clusters are needed to sample the bright end to obtain firm conclusions.
- We detect evidence of VLS for galaxies more luminous than  $m_3 + 0.5$ , brighter galaxies having lower velocities. Qualitatively, this result is similar to that found for local clusters, but we note and discuss minor differences, e.g. in the threshold value of the segregation.
- VLS concerns both red and blue galaxies. The latter finding still not reported in the literature, not even for local clusters.

Finally, we note that there is a strong correlation between  $\sigma_V$  based on red galaxies and  $\sigma_V$  based on blue galaxies and,

in particular, we find no significant bias in the High- $z$  sample. Although the appropriate mass calibration has to be determined, this result suggests that both red and blue galaxies can be used as tracers of the cluster mass distribution out to high redshift. This result has interesting implications for the cosmological application of the velocity dispersion measurements that the Euclid satellite will make possible by targeting H $\alpha$ -emitting, star-forming galaxies in its spectroscopic survey (e.g. Laureijs et al. 2011; Sartoris et al. 2016).

**Acknowledgements.** We thank the referee for useful comments. We thank P. Rosati for providing us data on XMMU J2235.3–2557. M.A., and A.B. and M.N. acknowledge financial support from PRIN-INAF 2014 1.05.01.94.02. M.G. acknowledges financial support from the University of Trieste through the program “Finanziamento di Ateneo per progetti di ricerca scientifica - FRA 2015”. S.B. acknowledges financial support from the PRIN-MIUR 201278X4FL grant and from the “InDark” INFN Grant. This research has made use of the NASA/IPAC Extragalactic Database (NED) which is operated by the Jet Propulsion Laboratory, California Institute of Technology, under contract with the National Aeronautics and Space Administration.

## References

- Abraham, R. G., Smecker-Hane, T. A., Hutchings, J. B., et al. 1996, *ApJ*, 471, 694
- Adami, C., Biviano, A., & Mazure, A. 1998, *A&A*, 331, 439
- Ashman, K. M., Bird, C. M., & Zepf, S. E. 1994, *AJ*, 108, 2348
- Beers, T. C., Flynn, K., & Gebhardt, K. 1990, *AJ*, 100, 32
- Bekki, K. & Couch, W. J. 2011, *MNRAS*, 415, 1783
- Biviano, A., Durret, F., Gerbal, D., et al. 1996, *A&A*, 311, 95
- Biviano, A. & Girardi, M. 2003, *ApJ*, 585, 205
- Biviano, A., Girardi, M., Giuricin, G., Mardirossian, F., & Mezzetti, M. 1992, *ApJ*, 396, 35
- Biviano, A. & Katgert, P. 2004, *A&A*, 424, 779
- Biviano, A., Katgert, P., Mazure, A., et al. 1997, *A&A*, 321, 84
- Biviano, A., Murante, G., Borgani, S., et al. 2006, *A&A*, 456, 23
- Biviano, A. & Poggianti, B. M. 2009, *A&A*, 501, 419
- Biviano, A., Rosati, P., Balestra, I., et al. 2013, *A&A*, 558, A1
- Borgani, S., Gardini, A., Girardi, M., & Gottlöber, S. 1997, *New A*, 2, 119
- Caldwell, N. & Rose, J. A. 1997, *AJ*, 113, 492
- Carlberg, R. G., Yee, H. K. C., Ellingson, E., et al. 1997, *ApJ*, 476, L7
- Carrasco, E. R., Cypriano, E. S., Neto, G. B. L., et al. 2007, *ApJ*, 664, 777
- Chincarini, G. & Rood, H. J. 1977, *ApJ*, 214, 351
- Colless, M. & Dunn, A. M. 1996, *ApJ*, 458, 435
- Crawford, S. M., Wirth, G. D., & Bershad, M. A. 2014, *ApJ*, 786, 30
- Danese, L., de Zotti, G., & di Tullio, G. 1980, *A&A*, 82, 322
- de Theije, P. A. M. & Katgert, P. 1999, *A&A*, 341, 371
- Demarco, R., Gobat, R., Rosati, P., et al. 2010, *ApJ*, 725, 1252
- Demarco, R., Rosati, P., Lidman, C., et al. 2007, *ApJ*, 663, 164
- Dolag, K., Bartelmann, M., Perrotta, F., et al. 2004, *A&A*, 416, 853
- Dressler, A. 1980, *ApJ*, 236, 351
- Dressler, A., Smail, I., Poggianti, B. M., et al. 1999, *ApJS*, 122, 51
- Ellingson, E., Yee, H. K. C., Abraham, R. G., Morris, S. L., & Carlberg, R. G. 1998, *ApJS*, 116, 247
- Ellingson, E., Yee, H. K. C., Abraham, R. G., et al. 1997, *ApJS*, 113, 1
- Fabricant, D. G., Bautz, M. W., & McClintock, J. E. 1994, *AJ*, 107, 8
- Fadda, D., Girardi, M., Giuricin, G., Mardirossian, F., & Mezzetti, M. 1996, *ApJ*, 473, 670
- Fassbender, R., Böhringer, H., Santos, J. S., et al. 2011, *A&A*, 527, A78
- Ferrari, C., Benoist, C., Maurogordato, S., Cappi, A., & Slezak, E. 2005, *A&A*, 430, 19
- Fukugita, M., Shimasaku, K., & Ichikawa, T. 1995, *PASP*, 107, 945
- Gerken, B., Ziegler, B., Balogh, M., et al. 2004, *A&A*, 421, 59
- Gioia, I. M., Henry, J. P., Mullis, C. R., Ebeling, H., & Wolter, A. 1999, *AJ*, 117, 2608
- Girardi, M., Biviano, A., Giuricin, G., Mardirossian, F., & Mezzetti, M. 1993, *ApJ*, 404, 38
- Girardi, M., Fadda, D., Giuricin, G., et al. 1996, *ApJ*, 457, 61
- Girardi, M., Mercurio, A., Balestra, I., et al. 2015, *A&A*, 579, A4
- Girardi, M., Rigoni, E., Mardirossian, F., & Mezzetti, M. 2003, *A&A*, 406, 403
- Goto, T. 2005, *MNRAS*, 359, 1415
- Haines, C. P., Pereira, M. J., Smith, G. P., et al. 2015, *ApJ*, 806, 101
- Halliday, C., Milvang-Jensen, B., Poirier, S., et al. 2004, *A&A*, 427, 397
- Hammer, F., Flores, H., Lilly, S. J., et al. 1997, *ApJ*, 481, 49
- Hernández-Fernández, J. D., Haines, C. P., Diaferio, A., et al. 2014, *MNRAS*, 438, 2186

- Hilton, M., Lloyd-Davies, E., Stanford, S. A., et al. 2010, *ApJ*, 718, 133
- Hwang, H. S. & Lee, M. G. 2008, *ApJ*, 676, 218
- Jørgensen, I. & Chiboucas, K. 2013, *AJ*, 145, 77
- Katgert, P., Mazure, A., Perea, J., et al. 1996, *A&A*, 310, 8
- Laureijs, R., Amiaux, J., Arduini, S., et al. 2011, *ArXiv e-prints* [[arXiv:1110.3193](#)]
- Lederman, W. 1984, *Handbook of applicable mathematics*. Vol.6,A: Statistics; Vol.6,B: Statistics (Wiley-Interscience Publication, Chichester)
- Lerchster, M., Seitz, S., Brimiouille, F., et al. 2011, *MNRAS*, 411, 2667
- Lubin, L. M., Oke, J. B., & Postman, M. 2002, *AJ*, 124, 1905
- Mahajan, S., Mamon, G. A., & Raychaudhury, S. 2011, *MNRAS*, 416, 2882
- Melnick, J. & Sargent, W. L. W. 1977, *ApJ*, 215, 401
- Milvang-Jensen, B., Noll, S., Halliday, C., et al. 2008, *A&A*, 482, 419
- Mohr, J. J., Geller, M. J., & Wegner, G. 1996, *AJ*, 112, 1816
- Moore, B., Katz, N., Lake, G., Dressler, A., & Oemler, A. 1996, *Nature*, 379, 613
- Moss, C. & Dickens, R. J. 1977, *MNRAS*, 178, 701
- Munari, E., Biviano, A., Borgani, S., Murante, G., & Fabjan, D. 2013, *MNRAS*, 430, 2638
- Owen, F. N., Ledlow, M. J., Keel, W. C., Wang, Q. D., & Morrison, G. E. 2005, *AJ*, 129, 31
- Owers, M. S., Nulsen, P. E. J., & Couch, W. J. 2011, *ApJ*, 741, 122
- Pisani, A. 1993, *MNRAS*, 265, 706
- Poggianti, B. M. 1997, *A&AS*, 122 [[astro-ph/9608029](#)]
- Postman, M., Lubin, L. M., & Oke, J. B. 1998, *AJ*, 116, 560
- Postman, M., Lubin, L. M., & Oke, J. B. 2001, *AJ*, 122, 1125
- Press, W. H., Teukolsky, S. A., Vetterling, W. T., & Flannery, B. P. 1992, *Numerical recipes in FORTRAN. The art of scientific computing* (Cambridge University Press, Cambridge)
- Ribeiro, A. L. B., Lopes, P. A. A., & Rembold, S. B. 2013, *A&A*, 556, A74
- Ribeiro, A. L. B., Lopes, P. A. A., & Trevisan, M. 2010, *MNRAS*, 409, L124
- Rines, K., Geller, M. J., Diaferio, A., & Kurtz, M. J. 2013, *ApJ*, 767, 15
- Rines, K., Geller, M. J., Kurtz, M. J., & Diaferio, A. 2003, *AJ*, 126, 2152
- Rines, K., Geller, M. J., Kurtz, M. J., & Diaferio, A. 2005, *AJ*, 130, 1482
- Rosati, P., Balestra, I., Grillo, C., et al. 2014, *The Messenger*, 158, 48
- Rosati, P., Tozzi, P., Gobat, R., et al. 2009, *A&A*, 508, 583
- Santos, J. S., Altieri, B., Valtchanov, I., et al. 2015, *MNRAS*, 447, L65
- Sarazin, C. L. 1986, *Reviews of Modern Physics*, 58, 1
- Sartoris, B., Biviano, A., Fedeli, C., et al. 2016, *MNRAS* [[arXiv:1505.02165](#)]
- Scoddeggio, M., Solanes, J. M., Giovanelli, R., & Haynes, M. P. 1995, *ApJ*, 444, 41
- Siegel, S. 1956, *Nonparametric statistics for the behavioral sciences* (McGraw-Hill Kogakusha, Tokyo)
- Sodré, Jr., L., Capelato, H. V., Steiner, J. E., & Mazure, A. 1989, *AJ*, 97, 1279
- Tammann, G. A. 1972, *A&A*, 21, 355
- Tanaka, M., Finoguenov, A., Kodama, T., et al. 2008, *A&A*, 489, 571
- Tran, K.-V. H., Franx, M., Illingworth, G. D., et al. 2007, *ApJ*, 661, 750
- Tran, K.-V. H., Papovich, C., Saintonge, A., et al. 2010, *ApJ*, 719, L126
- Vulcani, B., Aragón-Salamanca, A., Poggianti, B. M., et al. 2012, *A&A*, 544, A104
- Westra, E., Geller, M. J., Kurtz, M. J., Fabricant, D. G., & Dell’Antonio, I. 2010, *PASP*, 122, 1258
- White, S. D. M., Clowe, D. I., Simard, L., et al. 2005, *A&A*, 444, 365
- Whitmore, B. C., Gilmore, D. M., & Jones, C. 1993, *ApJ*, 407, 489
- Yee, H. K. C., Ellingson, E., & Carlberg, R. G. 1996, *ApJS*, 102, 269
- Zabludoff, A. I. & Franx, M. 1993, *AJ*, 106, 1314
- Ziparo, F., Popesso, P., Finoguenov, A., et al. 2014, *MNRAS*, 437, 458